nature physics

ARTICLES

PUBLISHED ONLINE: 4 SEPTEMBER 2011 | DOI: 10.1038/NPHYS2070

A single nitrogen-vacancy defect coupled to a nanomechanical oscillator

O. Arcizet[1]*, V. Jacques[2], A. Siria[3], P. Poncharal[3], P. Vincent[3] and S. Seidelin[1]

We position a single nitrogen-vacancy (NV) centre hosted in a diamond nanocrystal at the extremity of a SiC nanowire. This novel hybrid system couples the degrees of freedom of two radically different systems: a nanomechanical oscillator and a single quantum object. We probe the dynamics of the nano-resonator through time-resolved nanocrystal fluorescence and photon-correlation measurements, conveying the influence of a mechanical degree of freedom on a non-classical photon emitter. Moreover, by immersing the system in a strong magnetic field gradient, we induce a magnetic coupling between the nanomechanical oscillator and the NV electronic spin, providing nanomotion readout through a single electronic spin. Spin-dependent forces inherent to this coupling scheme are essential in a variety of active cooling and entanglement protocols used in atomic physics, and should now be within the reach of nanomechanical hybrid systems.

Owing to recent developments in cavity opto- and electromechanics[1–3], it is now realistic to envisage the observation of macroscopic mechanical oscillators cooled by active or traditional cryogenic techniques close to their ground state of motion. This conceptually elegant accomplishment would give access to a vast playground for physicists if the resonator wavefunction could be coherently manipulated such as to create, maintain and probe Fock or other non-classical states. It would provide a remarkable opportunity to extend the pioneering experiments with trapped ions[4] to encompass macroscopic objects. However, standard continuous measurement techniques used to actively cool and probe the resonator[5], when used to manipulate its quantum state, tend to blur its non-classical nature. An attractive alternative consists in interfacing the mechanical degrees of freedom with a single quantum object, such as a 2-level system with a quantum state that can be externally controlled[6–11]. Successful realization of this type of coupling between a nanomechanical oscillator in the quantum regime and a phase qubit was recently reported[12] and motivates the development of similar hybrid quantum systems presenting extended coherence times at room temperature that are compatible with continuous measurement approaches.

Here we report a first step in this direction by coupling a nanomechanical oscillator to a single negatively-charged nitrogen-vacancy (NV) defect hosted in a diamond nanocrystal attached to its extremity (Fig. 1a). In that context, the NV defect seems to be an attractive quantum system, both for its optical and electronic spin properties. Indeed, perfect photostability at room temperature makes the NV defect a robust and practical single-photon source[13,14]. Moreover, the NV defect ground state is a spin triplet (Fig. 1b) that can be initialized and read-out by optical means, and manipulated by resonant microwave excitation with an unprecedented coherence time for a solid-state system under ambient conditions[15,16]. Such properties are at the heart of diamond-based quantum information processing[17–21] and ultrasensitive magnetometry, where the spin is used as an atomic-sized magnetic sensor[22–24]. These results make the NV defect an appealing candidate for interfacing a nanomechanical oscillator: once immersed in a strong magnetic field gradient, an efficient coupling between the NV defect electronic spin and the nanoresonator position can be achieved. Furthermore, this novel hybrid system has the potential to reach the strong coupling regime, as already envisaged in refs 8,25.

In the following, we first show that the nanomechanical oscillator dynamics can be probed using the NV centre as a single-photon source, illustrating a resonant optomechanical coupling that does not suffer from the usual reduction in strength typically observed while optically interacting with sub-wavelength sized resonators. Furthermore, we provide clear spectroscopic evidence of the mechanical degree of freedom by magnetic coupling of the spin to the nanoresonator position, demonstrating spin-mediated readout of the oscillator dynamics.

The nanomechanical oscillator consists of a SiC nanowire attached to the extremity of a conducting tungsten tip (Fig. 1). SiC nanowires offer compelling features for nanomechanical oscillators, providing a low mass system with a high mechanical quality factor, a relatively high vibration frequency and a large spreading of the zero-point energy wave function. For a 10 μm long and 50 nm diameter nanowire, with an effective mass of $M_{\mathrm{eff}} = 16$ fg, the vibration frequency reaches $\Omega_{\mathrm{m}}/2\pi \equiv 1/T = 1$ MHz with a spring constant $k = 1/M_{\mathrm{eff}}\Omega_{\mathrm{m}}^2 = 700\,\mu\mathrm{N\,m^{-1}}$, corresponding to a room temperature Brownian motion of 3 nm r.m.s. (root mean square) and a groundstate wave function spreading of $\Delta x^q = \sqrt{\hbar/(2M_{\mathrm{eff}}\Omega_{\mathrm{m}})} \approx 0.7$ pm. The nanomechanical oscillator can be efficiently driven to large oscillation amplitudes (several μm), as shown in Fig. 2a. Resonators with a mechanical quality factor (Q) above 10,000 were measured in vacuum in the transmission electron microscope, and even larger values can be achieved in similar devices[26].

A diamond nanocrystal hosting a single NV defect is attached to the free extremity of the oscillator and fluorescence is detected using a confocal microscope, as shown in Fig. 1 (see Methods). When the hybrid system is set into motion, its extremity oscillates back and forth across the optical spot, thus modulating the overlap with the optical detection volume (Fig. 2b). As the emitter can be pumped and a photon detected only when located within this volume, the

[1]Institut Néel, CNRS et Université Joseph Fourier, BP 166, F-38042 Grenoble Cedex 09, France, [2]Laboratoire de Photonique Quantique et Moléculaire, 94235 Cachan, France, [3]Laboratoire de Physique de la Matière Condensée et Nanostructures, CNRS and Université Claude Bernard, 69622 Villeurbanne, France. *e-mail: olivier.arcizet@grenoble.cnrs.fr.

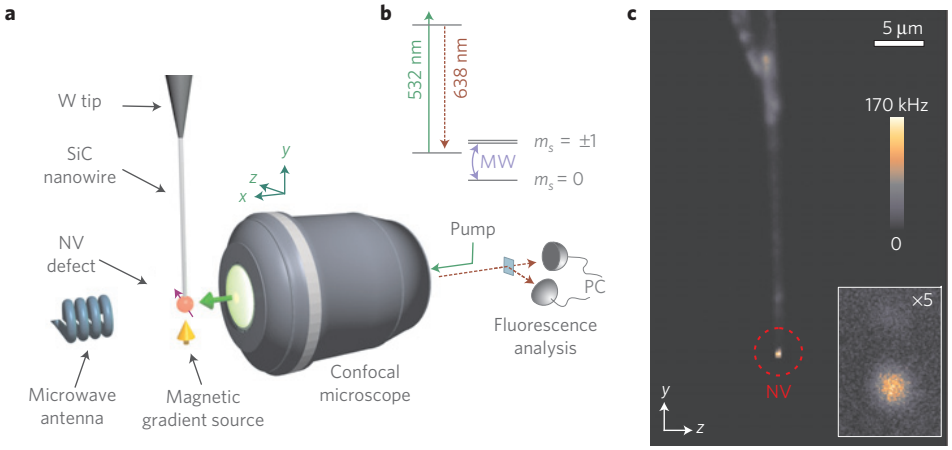

Figure 1 | The hybrid system. a, A confocal microscope monitors the fluorescence of a single NV defect hosted in a diamond nanocrystal positioned at the extremity of a SiC nanowire. A microwave (MW) antenna is used to manipulate the NV electronic spin, while a micro-fabricated magnetic structure approached in the vicinity of the suspended NV centre generates a strong magnetic field gradient. **b**, Simplified electronic structure of the NV centres at zero magnetic field. **c**, Fluorescence map of the system recorded with the confocal microscope while scanning the objective position. The isolated bright spot circled in red corresponds to the fluorescence of a single NV centre. Inset: zoom on the nanowire extremity.

fluorescence rate therefore provides a simple detection technique for the resonator dynamics (Fig. 2c). A time-resolved fluorescence measurement synchronized with the piezo-driving voltage (Fig. 2d) probes the oscillator dynamics across the optical spot. From this, the oscillation amplitude and direction can be determined and the piezo-driving efficiency calibrated (of the order of 200 nm V^{-1} for the 625 kHz mode considered here). Note that, in this experiment, the NV centre serves as a probe of the nanoresonator dynamics, and the recoil displacements, $\delta x^{\mathrm{rec}} = h/(\lambda M_{\mathrm{eff}}\Omega_{\mathrm{m}}) \approx 10$ am, due to single-photon emission ($\lambda = 638$ nm) are negligible compared with Δx^{q}, which is equivalent to the Lamb–Dicke regime[4].

The mechanical degree of freedom given to the single quantum emitter is further elucidated by recording the histogram of the time delays between two consecutive single-photon detections using a standard Hanbury-Brown–Twiss (HBT) interferometer. After normalization to a Poissonnian statistics[27], the recorded histogram is equivalent to a measurement of the second-order autocorrelation function $g^{(2)}(\tau)$. For an oscillator at rest, a pronounced anticorrelation effect is observed ($g^{(2)}(0) \approx 0.3$), as expected for a single quantum emitter (Fig. 2e). This shape is strongly modified when the emitter is in motion. Although the anticorrelation effect is still observed at zero delay, additional periodic drops appear, reflecting the time intervals spent outside the detection volume, as usually observed for the $g^{(2)}(\tau)$ function recorded under pulsed excitation. The regime presented here corresponds to a slow oscillator, driven at amplitudes for which the time required to cross the optical detection volume—corresponding to the width of the peaks in the autocorrelation trace—remains long compared with the single-emitter lifetime (12 ns). The photon emission probability of the single emitter therefore adiabatically follows the spatial variations of the pump intensity as it traverses the optical spot. A different and equally interesting regime arises in the situation where the illumination duration is comparable to the emitter lifetime. This can be readily reached; for example with a 10-MHz oscillator, driven at 1 µm oscillation amplitudes.

Together, the results presented above opens the road towards a wide range of experiments merging the fields of single-emitter quantum optics and optomechanics.

The second part of this letter demonstrates the coupling between the nanomechanical oscillator position and the electronic spin of the NV defect. The ground state is a spin triplet $S = 1$, the degeneracy of which is lifted to 2.8 GHz by spin–spin interactions in the absence

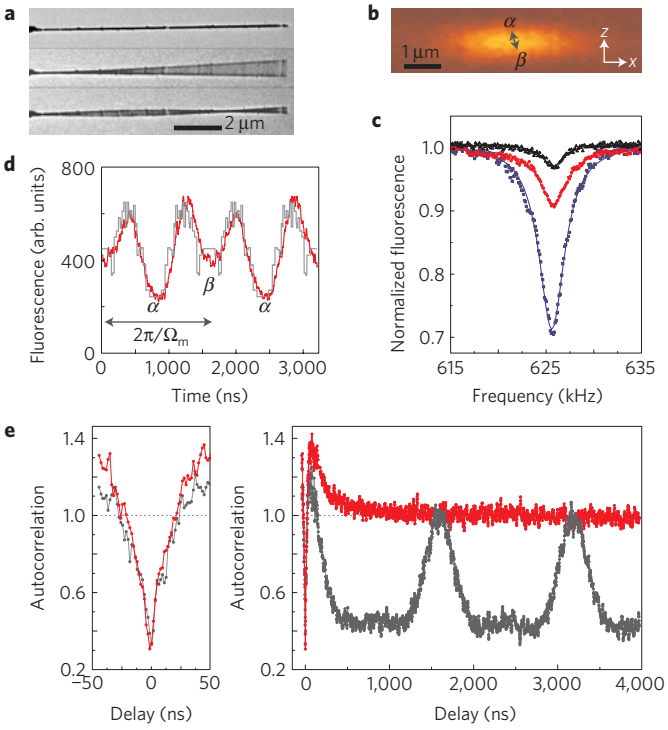

Figure 2 | A single quantum emitter with a mechanical degree of freedom. **a**, Transmission electron microscope images of a SiC nanowire at rest (top) and oscillating under electrostatic excitation at the frequency of its two lower eigenmodes (654 and 4,887 kHz). **b**, Fluorescence map of the suspended NV within the optical spot in its oscillation plane. **c**, Detection of piezo-driven nanomechanical resonances by monitoring the mean NV fluorescence as a function of the piezo-driving frequency for increasing amplitudes (from top to bottom: 50, 100 and 200 nm at resonance). **d**, In red, time-resolved fluorescence of the suspended NV centre driven at 625 kHz. Its comparison to the static fluorescence map of **b** allows one to extract the oscillation parameters (direction, amplitude and turning points (α, β)), represented by an arrow in **b** and corresponding to the grey trace in **d**. **e**, Photon correlation measurements, recorded using a standard HBT setup, of the suspended single NV centre at rest (red) and oscillating with a 200 nm amplitude at 625 kHz (black) (left: zoom on short time delays).

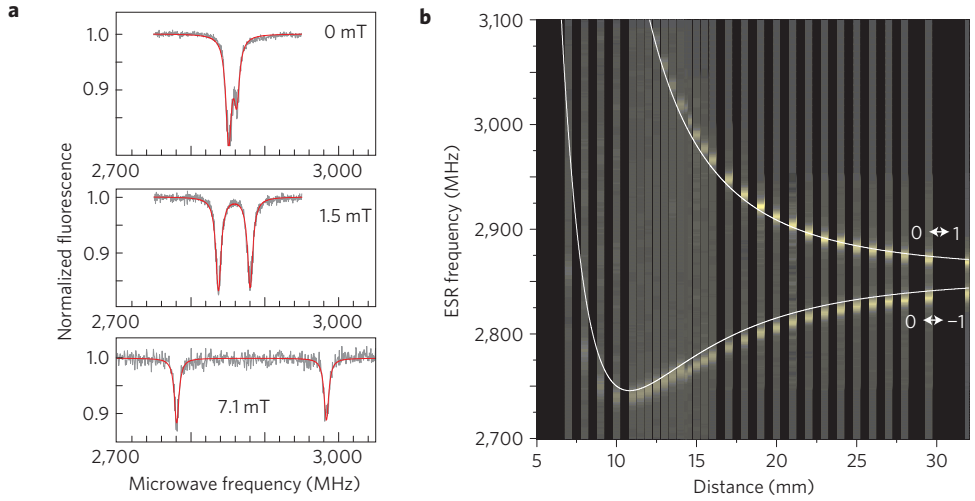

Figure 3 | Optically detected ESR measured on the suspended NV centre at rest. a, Zeeman shift of the ESR frequencies for increasing values of the magnetic field applied along an arbitrary direction. The red curves are double Lorentzian fits to the data. **b**, Typical map of the ESR resonances as a function of the distance to a calibrated magnet. The fit (white lines) gives the orientation of the NV axis.

of static magnetic fields (Fig. 1b; ref. 28). Radiative transition selection rules associated with the spin state quantum number provide a high degree of spin polarization in the $m_S = 0$ substate through optical pumping. In addition, the photoluminescence intensity of the NV defect is significantly higher when the $m_S = 0$ state is populated[28]. Owing to this spin-dependent fluorescence rate, electron spin resonances (ESR) can be optically detected[15,29]. More precisely, as shown in Fig. 3a, when the suspended single NV defect, initially prepared in the $m_S = 0$ state through optical pumping, is driven to the $m_S = \pm 1$ spin states by applying a resonant microwave field, a dip in the photoluminescence signal is observed. The orientation of the suspended NV defect was determined by measuring the Zeeman shift of the ESR frequencies as a function of the orientation and magnitude of a calibrated static magnetic field (Fig. 3b). The latter were subsequently fitted according to the eigenvalues of the ground-state spin Hamiltonian given by $H_{\rm spin} = DS_Z^2 + E(S_X^2 - S_Y^2) + g\mu_B \mathbf{B}\cdot\mathbf{S}$, where D and E are the zero-field splitting parameters, Z the NV defect quantization axis, g its g-factor ($\approx$2), and μ_B the Bohr magneton. The NV axis was found to be aligned (within 5°) with the oscillation trajectory of a 625 kHz mode of the nanoresonator, coinciding with the z axis of Fig. 1a.

To magnetically couple the electronic spin and the nanoresonator position we applied a strong magnetic field gradient to the suspended NV, rendering its electronic spin energy dependent on the oscillator position z. To this end, an in-house patterned magnetic structure[30] with an extended homogeneity of the field gradient was micro-positioned in the vicinity of the suspended NV. The magnetic field was aligned with the NV axis to maintain a high ESR contrast, and the position optimized to find a gradient that was homogeneous along the oscillating NV trajectory. A prominent signature of the coupling is the modification of the ESR profile when the oscillator is set in motion. As the oscillation frequency of the mode considered here (625 kHz) is smaller than the ESR linewidth (power broadened to a half-width at half-maximum (HWHM) of $\Gamma_s/2\pi = 7$ MHz), we can consider that the electron spin adiabatically follows the Zeeman-shifted resonances. The evidence of magnetic coupling between the nanomechanical oscillator position and the NV electronic spin is illustrated in Fig. 4b, where one can observe a motional ESR broadening followed by a characteristic splitting at stronger oscillation amplitudes (δz), the shape of which reflects the harmonic oscillation turning points.

For a NV axis oriented along the oscillation direction and magnetic field ($z \simeq Z$), which holds true in our system, the system is formally described by the coupling Hamiltonian $g\mu_B \nabla B\, S_Z\, z$. In this case, we can approximate the magnetic coupling by a scalar description. Accordingly, the data from Fig. 4b were fitted with the function

$$\Lambda(f, \delta z) = \frac{1}{T}\int_0^T \mathfrak{L}\left(f, f_0 - \frac{g\mu_B}{h} B(\delta z \cos\Omega_m t)\right) {\rm d}t$$

where $\mathfrak{L}(f, f_{\rm ESR})$ is the unperturbed ESR resonance shape, which for simplicity is supposed to be Lorentzian (half-width $\Gamma_s/2\pi$). $B(z)$ is the magnetic field along the NV trajectory, approximated by $B(z) = B_0 + ({\rm d}B/{\rm d}z)z + ({\rm d}^2B/{\rm d}z^2)z^2$, the coefficients of which are the only free parameters in the fitting procedure. This model is in good agreement with experimental data, even at strong oscillation amplitudes. The effective spin resonance half-width, defined as $(1/2\pi)\sqrt{\Gamma_s^2 + ((g\mu_B/\hbar)({\rm d}B/{\rm d}z)\delta z)^2}$, is then plotted as a function of the calibrated oscillation amplitude δz in Fig. 4c (in red for the data set presented in 4b, in blue and grey for different gradients). The plot allows one to verify the consistency of each data set and to extract the magnetic field gradient, which amounts to 6,700 T m^{-1} for the data shown in Fig. 4b. This value and the mean magnetic field ($B_0 = 90$ mT), also obtained from the fit, are in good agreement with both static measurements of the field spatial profile obtained by locally displacing the magnetic structure, as well as with simulations[30]. The mechanical quality factor (damped to $Q = 150$ in air) is obtained by sweeping the driving frequency across the resonance (Fig. 4d).

Having observed how the nanomotion is imprinted on the electronic spin dynamics, a question that naturally arises is whether the NV electronic spin can affect the nanoresonator dynamics[31]. The realization of this reverse interaction would enable cooling of the nanoresonator or preparation of non-classical mechanical states through spin-dependent forces[4]. For a magnetic field gradient of 10^5 T m^{-1}, the change in the spin-dependent force exerted on the nanomechanical oscillator from one spin state to another amounts to $g\mu_B \nabla B \approx 2$ aN. This order of magnitude is comparable to the thermal-noise-limited force sensitivity of the nanoresonator, $\sqrt{2M_{\rm eff}\Omega_m k_B T/Q} \approx 9\,{\rm aN}/\sqrt{\rm Hz}$, expected at room temperature for the parameters previously used and the vacuum $Q = 10{,}000$. Resolving the Brownian motion thus gives a reasonable metric for the sensitivity required to detect the spin dynamics. The

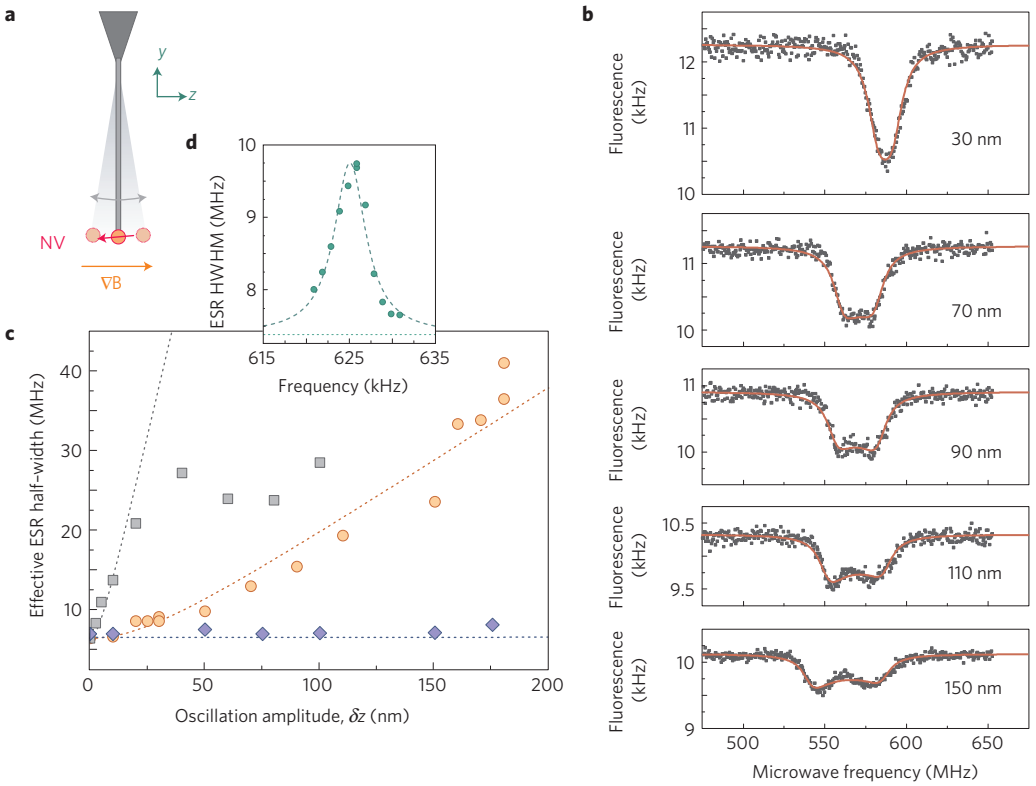

Figure 4 | Magnetic coupling of the NV electronic spin to the nanomotion observed on the $m_S = 0$ to $m_S = -1$ transition. a, Schematics of the experiment. **b**, ESR obtained for an increasing oscillation amplitude at $\Omega_m/2\pi = 625$ kHz. The red line is a fit (see main text) allowing one to extract the effective ESR half-width, which is reported in **c** (circles) as a function of the oscillation amplitude (δz). **c**, Various magnetic field gradients (0.1, 6,700 and 45,000 T m^{-1}) were explored, corresponding to different distances above the magnetic structure (1,000, 15 and 2 μm (blue, red, grey)), allowing one to tune the NV-oscillator coupling strength. The deviation from the model observed at large driving amplitudes in the strongest gradient case (grey squares) is a consequence of the reduced gradient homogeneity at short distances from the structure. **d**, Effective ESR half-width as a function of the driving frequency, for a 4,500 T m^{-1} gradient and a resonant oscillation amplitude of 50 nm.

corresponding room temperature thermal noise at resonance (1 MHz) amounts to approximately 100 pm/$\sqrt{\text{Hz}}$, an order of magnitude that can be easily detected using simple optical means despite the sub-wavelength size of the resonator[32–35]. Furthermore, to probe spin dynamics with the nanoresonator, spin coherence has to be preserved over several mechanical oscillations. The so-called resolved sideband regime ($\Omega_m > \Gamma_s$) is within reach when working with shorter nanowires and increased spin coherence times, and is also of importance when exploring the avenues for probing and cooling the nanomechanical oscillator down to its quantum ground state through single spin manipulations[8,36].

These results represent a clear quantitative signature of the nanoresonator motion directly imprinted on the electronic spin dynamics through magnetic coupling. Long-lived electronic spins coupled to nanomechanical oscillators represent a promising hybrid system for which both components can independently be monitored and controlled. This, combined with the single photon source character of the suspended NV defect, paves the way towards single photon optomechanics.

Methods

Nanowire functionalization. A diamond nanocrystal hosting a single NV defect is attached to the free extremity of the oscillator during a piezo-controlled immersion into a commercial solution of 50-nm-diameter diamond nano-crystals. The adhesion efficiency is markedly increased under focussed laser illumination, as a result of the increased convection combined with an optical tweezer mechanism. As the solution meniscus size remains comparable to the nanowire diameter, it is possible to functionalize just the very extremity of the nanowire, with a subsequent focussed ion beam cut allowing final adjustments. This method allows the efficient and robust positioning of a single NV centre at the extremity of a nanowire and works reliably over a wide variety of resonator sizes and materials, including carbon and boron nitride nanotubes.

Experimental setup. The NV centre is excited through a ×100 long working distance microscope objective (generating an approximately 450 nm diameter optical spot). The fluorescence is collected by the same objective and detected on avalanche photodiodes. The objective is mounted on a fast Physik Instrument XYZ piezo stage to localize the suspended NV defect (Fig. 1c). A tracking program continuously maintains the detection spot on the single emitter. A fast piezoelectric module positioned on top of the STM tip drives the nanomechanical oscillator while a micro-antenna generates the microwave field used to manipulate the NV electronic spin.

Received 23 March 2011; accepted 13 July 2011; published online 4 September 2011

References

1. Aspelmeyer, M. & Schwab, K. C. Focus on mechanical systems at the quantum limit. *New J. Phys.* **10,** 095001 (2008).
2. Kippenberg, T. J. & Vahala, K. J. Cavity optomechanics: Back-action at the mesoscale. *Science* **321,** 1172–1176 (2008).
3. Schwab, K. C. & Roukes, M. L. Putting mechanics into quantum mechanics. *Phys. Today* **58,** 36–42 (July, 2005).
4. Blatt, R. & Wineland, D. J. Entangled states of trapped atomic ions. *Nature* **453,** 1008–1015 (2008).
5. Braginsky, V. B. & Khalili, F. Y. in *Quantum Measurement* (Cambridge Univ. Press, 1992).
6. Wilson-Rae, I., Zoller, P. & Imamoglu, A. Laser cooling of a nanomechanical resonator mode to its quantum ground state. *Phys. Rev. Lett.* **92,** 075507 (2004).
7. Hammerer, K. *et al.* Strong coupling of a mechanical oscillator and a single atom. *Phys. Rev. Lett.* **103,** 063005 (2009).
8. Rabl, P. *et al.* Strong magnetic coupling between an electronic spin qubit and a mechanical oscillator. *Phys. Rev. B* **79,** 041302 (2009).
9. Hunger, D. *et al.* Resonant coupling of a Bose–Einstein condensate to a micromechanical oscillator. *Phys. Rev. Lett.* **104,** 143002 (2010).

10. LaHaye, M. D., Suh, J., Echternach, P. M., Schwab, K. C. & Roukes, M. L. Nanomechanical measurements of a superconducting qubit. *Nature* **459,** 960–964 (2009).
11. Bennett, S. D., Cockins, L., Miyahara, Y., Grütter, P. & Clerk, A. A. Strong electromechanical coupling of an atomic force microscope cantilever to a quantum dot. *Phys. Rev. Lett.* **104,** 017203 (2010).
12. O'Connell, A. D. *et al.* Quantum ground state and single-phonon control of a mechanical resonator. *Nature* **464,** 697–703 (2010).
13. Kurtsiefer, C., Mayer, S., Zarda, P. & Weinfurter, H. Stable solid-state source of single photons. *Phys. Rev. Lett.* **85,** 290–293 (2000).
14. Brouri, R., Beveratos, A., Poizat, J-P. & Grangier, P. Photon antibunching in the fluorescence of individual color centers in diamond. *Opt. Lett.* **25,** 1294–1296 (2000).
15. Jelezko, F., Gaebel, T., Popa, I., Gruber, A. & Wrachtrup, J. Observation of coherent oscillations in a single electron spin. *Phys. Rev. Lett.* **92,** 076401 (2004).
16. Balasubramanian, G. *et al.* Ultralong spin coherence time in isotopically engineered diamond. *Nature Mater.* **8,** 383–387 (2009).
17. Gurudev Dutt, M. V. *et al.* Quantum register based on individual electronic and nuclear spin qubits in diamond. *Science* **316,** 1312–1316 (2007).
18. Neumann, P. *et al.* Multipartite entanglement among single spins in diamond. *Science* **320,** 1326–1329 (2008).
19. Buckley, B. B., Fuchs, G. D., Bassett, L. C. & Awschalom, D. D. Spin-light coherence for single-spin measurement and control in diamond. *Science* **330,** 1212–1215 (2010).
20. Togan, E. *et al.* Quantum entanglement between an optical photon and a solid-state spin qubit. *Nature* **466,** 730–734 (2010).
21. Neumann, P. *et al.* Single-shot readout of a single nuclear spin. *Science* **329,** 542–544 (2010).
22. Maze, J. R. *et al.* Nanoscale magnetic sensing with an individual electronic spin in diamond. *Nature* **455,** 644–647 (2008).
23. Balasubramanian, G. *et al.* Nanoscale imaging magnetometry with diamond spins under ambient conditions. *Nature* **455,** 648–651 (2008).
24. de Lange, G., Ristè, D., Dobrovitski, V. V. & Hanson, R. Single-spin magnetometry with multipulse sensing sequences. *Phys. Rev. Lett.* **106,** 080802 (2011).
25. Rabl, P. *et al.* A quantum spin transducer based on nanoelectromechanical resonator arrays. *Nature Phys.* **6,** 602–608 (2010).
26. Perisanu, S. *et al.* High Q factor for mechanical resonances of batch-fabricated SiC nanowires. *Appl. Phys. Lett.* **90,** 043113 (2007).
27. Beveratos, A. *et al.* Room temperature stable single-photon source. *Eur. Phys. J. D* **18,** 191–196 (2002).
28. Manson, N. B., Harrison, J. P. & Sellars, M. J. Nitrogen-vacancy center in diamond: Model of the electronic structure and associated dynamics. *Phys. Rev. B* **74,** 104303 (2006).
29. Gruber, A. *et al.* Scanning confocal optical microscopy and magnetic resonance on single defect centers. *Science* **276,** 2012–2014 (1997).
30. Kustov, M. *et al.* Magnetic characterization of micropatterned Nd–Fe–B hard magnetic films using scanning hall probe microscopy. *J. Appl. Phys.* **108,** 063914 (2010).
31. Rugar, D., Budakian, R., Mamin, H. J. & Chui, B. W. Single spin detection by magnetic resonance force microscopy. *Nature* **430,** 329–332 (2004).
32. Sanii, B. & Ashby, P. D. High sensitivity deflection detection of nanowires. *Phys. Rev. Lett.* **104,** 147203 (2010).
33. Favero, I. *et al.* Fluctuating nanomechanical system in a high finesse optical microcavity. *Opt. Express* **17,** 12813–12820 (2009).
34. Anetsberger, G. *et al.* Near-field cavity optomechanics with nanomechanical oscillators. *Nature Phys.* **5,** 909–914 (2009).
35. Regal, C. A., Teufel, J. D. & Lehnert, K. W. Measuring nanomechanical motion with a resonant microwave interferometer. *Nature Phys.* **4,** 555–560 (2008).
36. Rabl, P. Cooling of mechanical motion with a two-level system: The high-temperature regime. *Phys. Rev. B* **82,** 165320 (2010).

Acknowledgements

We acknowledge J. Jarreau, C. Hoarau, D. Lepoitevin, J. F. Motte, P. Brichon, N. Dempsey, O. Fruchart, F. D. Bouchiat, D. Givord, E. Gheeraert, O. Mollet, A. Drezet, J. F. Roch, S. Huant and J. Chevrier for technical support, experimental assistance and discussions. This work is funded by the European Commission (Marie Curie ERG within FP7) and the Agence Nationale de la Recherche (projects QNAO and QNOM).

Author contributions

All authors contributed to all aspects of this work.

Additional information

The authors declare no competing financial interests. Reprints and permissions information is available online at http://www.nature.com/reprints. Correspondence and requests for materials should be addressed to O.A.